

# Suppression of stimulated Raman scattering in a high power Yb-doped fiber amplifier using a W-type core with fundamental mode cut-off

J. Kim, P. Dupriez, C. Codemard, J. Nilsson, and J. K. Sahu

*Optoelectronics Research Centre, University of Southampton, Southampton, SO17 1BJ, UK*  
[jsk@orc.soton.ac.uk](mailto:jsk@orc.soton.ac.uk)

**Abstract:** We demonstrate the suppression of stimulated Raman scattering in a high power, single-mode Yb-doped fiber amplifier using a W-type core structure. Raman-scattered light is not guided by the core. The amplifier consists of a master oscillator power amplifier (MOPA) system, seeded with 103 ps pulses at 32 MHz repetition rate in the final amplification stage. An average output power of 53 W, which corresponds to 13 kW of peak power, was achieved in the 23 m long W-type double-clad fiber without any significant loss of power due to transfer from the signal wavelength at 1060 nm to the Raman Stokes wavelength at 1114 nm and amplified spontaneous emission from Yb-ions at longer wavelengths (~1070 nm). The power conversion efficiency at 1060 nm was 80% with respect to the absorbed pump power.

©2006 Optical Society of America

**OCIS codes:** (060.2280) Fiber design and fabrication; (060.2320) Fiber optics amplifiers and oscillators; (060.4370) Nonlinear optics, fibers; (140.3510) Lasers, fiber; (140.3570) Lasers, single-mode.

---

## References and links

1. Y. Jeong, J. K. Sahu, D. N. Payne, and J. Nilsson, "Ytterbium-doped large-core fiber laser with 1.36kW continuous-wave output power," *Opt. Express* **12**, 6088-6092 (2004).
2. V. Gapontsev, "2kW single mode output from the fiber laser," presented at Photonic West 2005, San Jose, USA, Jan 21- 26 (2005).
3. P. Dupriez, A. Piper, A. Malinowski, J. K. Sahu, M. Ibsen, Y. Jeong, L. M. B. Hickey, M. N. Zervas, J. Nilsson, and D. J. Richardson, "321 W average power 1 GHz, 20 ps 1060 nm pulsed fiber MOPA source," presented at OFC 2005, Anaheim, USA 6-11 Mar 2005 (Postdeadline).
4. C. D. Brooks and F. D. Teodoro, "1-mJ energy, 1-MW peak-power, 10-W average-power, spectrally narrow, diffraction-limited pulses from a photonic-crystal fiber amplifier," *Opt. Express* **13**, 8999-9002 (2005).
5. F. D. Teodoro, J. P. Koplow, S. W. Moore, and D. A. V. Kliner, "Diffraction-limited, 300-kW-peak-power pulses from a Yb-doped fiber amplifier," in *Proc. CLEO 2002*, Long Beach, USA, 19-24 May 2002 Technical Digest vol.1 pp592-593
6. J. A. Alvarez-Chavez, A. B. Grudinin, J. Nilsson, P. W. Turner, and W. A. Clarkson, "Mode selection in high power cladding pumped fiber lasers with tapered section," presented at CLOE/QELS 1999 Baltimore 23-28 May 1999 CWE7.
7. J. Limpert, A. Liem, H. Zellmer, and A. Tünnermann, "500 W continuous-wave fiber laser with excellent beam quality" *Electron. Lett.* **39**, 645-647 (2003).
8. N. S. Platonov, D. V. Gapontsev, V. P. Gapontsev, and V. Shumilin, "135 W CW fiber laser with perfect single mode output" in *Proc. CLEO 2002*, Long Beach, USA, 19-24 May 2002 (postdeadline paper CPDC3).
9. E. A. Kuzin, G. Beltran-Perez, M. A. Basurto-Pensado, R. Rojas-Laguna, J. A. Andrade-Lucio, M. Torres-Cisneros, and E. Alvarado-Mendez, "Stimulated Raman scattering in a fiber with bending loss" *Opt. Commun.* **169**, 87-91 (1999).
10. P. D. Dragic, "Suppression of first order stimulated Raman scattering in erbium-doped fiber laser based LIDAR transmitters through induced bending loss" *Opt. Commun.* **250**, 403-410 (2005).
11. L. Zenteno, J. Wang, D. Walton, B. Ruffin, M. Li, S. Gray, A. Crowley, and X. Chen, "Suppression of Raman gain in single-transverse-mode dual-hole-assisted fiber" *Opt. Express* **13**, 8921-8926, (2005).
12. J. M. Fini, "Bend-resistant design of conventional and microstructure fibers with very large mode area," *Opt.*

- Express **14**, 69-81 (2006).
13. V. I. Neves and A. S. C. Fernandes, "Modal characteristics for W-type and M-type dielectric profile fibres", *Micro. & Opt. Tech. Lett.* **22**, 398-405 (1999).
  14. D. B. S. Soh, S. Yoo, J. Nilsson, J. K. Sahu, K. Oh, S. Baek, Y. Jeong, C. A. Codemard, P. Dupriez, J. Kim, and V. Philippov "Neodymium-doped cladding pump aluminosilicate fiber laser tunable in the 0.9 $\mu$ m wavelength range", *IEEE J. Quantum Electron.* **40**, 1275-1282, (2004).
  15. T. J. Kane, G. Keaton, M. A. Arbore, D. R. Balsley, J. F. Black, J. L. Brooks, M. Byer, L. A. Eyres, M. Leonardo, J. J. Morehead, C. Rich, D. J. Richard, L. A. Smoliar, and Y. Zhou, "3-Watt blue source based on 914-nm Nd:YVO<sub>4</sub> passively-Q-switched laser amplified in cladding-pumped Nd: fiber", presented at Adv. Solid-State Photonics Santa Fe, NM, USA, February 2-5, 2004, paper MD7.
  16. R. G. Smith, "Optical power handling capacity of low loss optical fibers as determined by stimulated Raman and Brillouin scattering" *Appl. Opt.* **11**, 2489-2494 (1972).
  17. G. P. Agrawal, *Nonlinear fiber optics*, (San Diego, Academic press, 3<sup>rd</sup> edition, 2001).
  18. L. G. Cohen, D. Marcuse, and W. L. Mammel, "Radiating leak-mode losses in single-mode lightguides with depressed-index claddings" *IEEE J. Quantum Electron.* **QE-18**, 1467-1472 (1982).

## 1. Introduction

Cladding-pumping enables fiber lasers to reach output power levels where they can compete with conventional bulk solid state lasers in many applications such as micro-machining, welding and materials processing. The continuous wave (CW) output power of high brightness cladding-pumped ytterbium (Yb) doped fiber lasers has already reached the kW-level [1-2]. Moreover, fiber-based master oscillator – power amplifier (MOPA) sources show the potential to scale up the average output power of more sophisticated waveforms, such as picosecond pulses [3]. For those, fiber nonlinearities become an important issue. Stimulated Raman scattering (SRS) is a main obstacle for power scaling of pulsed fiber systems. It can occur in the laser or amplifier itself as well as in any delivery fiber. To date, most high power pulsed fiber sources use a large low-NA core and a relatively short fiber. The resulting reduction of the power density and the interaction length mitigate SRS and other nonlinear effects. This has enabled pulsed fiber amplifiers to be scaled to the MW level and beyond [4-5]. While large cores eventually lead to a multimode output beam and so a degraded beam quality, the beam quality obtained with a multimode core can be improved by filtering out the higher order modes, e.g., by tapering the fiber or coiling a low-NA fiber [6-7]. However, these methods have their limitations and may be difficult to implement in a robust and reliable manner. In practice, the acceptance of mode-filtered and short fiber devices has been slow in commercial products. Furthermore, those methods to high peak powers and diffraction-limited output are difficult to implement in delivery fibers, which is another important application.

Hence, a single-mode core still remains an obvious choice for high beam quality. However, a single-mode (i.e., small) core requires a long fiber in the cladding-pumped configuration, because of the relatively low pump absorption due to the large area ratio between the inner cladding (pump waveguide) and the Yb-doped core. The resulting strong interaction of the optical field with the small core over a long fiber will reduce the SRS threshold significantly [8]. The SRS threshold becomes proportional to the inverse of the fourth power of the core diameter. Therefore, the suppression of SRS is required in order to scale up the output power in a small-core robustly single-mode system. Recently, several groups have demonstrated SRS suppression through bending the single-mode fiber and thus by introducing wavelength dependent loss [9-10]. However, such fibers with normal step index structure will introduce a significant amount of loss at the signal wavelength too, because of the relatively slow dependence of bending loss on the wavelength. Recently, a dual hole assisted fiber with the fundamental mode cut-off has been suggested for the suppression of Raman gain [11]. This fiber can provide a sharper cut-off characteristic, but the fiber was passive rather than active, and no amplifier or laser results were presented.

In this paper, a W-type fiber designed with a true fundamental mode cut-off is proposed for SRS suppression in a high peak power fiber MOPA source with a single-mode output. We

demonstrate 103 ps, 32 MHz, 53 W average output power at 1060 nm in a small and single-mode core without SRS. The peak power was 13 kW. The use of a small core fiber, readily compatible with existing fiber technology, would allow for a compactly packaged, all-fiber high power source.

## 2. SRS suppression: approach and simulations

In a co-pumped YDFA, the power evolution of the pump ( $P_p$ ), signal ( $P_s$ ) and Raman Stokes ( $P_R$ ) (the lower indices, P, S and R indicates the pump, the signal and Raman Stokes respectively) is determined by the following coupled differential equations in the steady state,

$$\frac{dP_p}{dz} = [(\sigma_p^a + \sigma_p^e)N_2 - \sigma_p^a]N\Gamma_p P_p, \quad (1)$$

$$\frac{dP_s}{dz} = [(\sigma_s^a + \sigma_s^e)N_2 - \sigma_s^a]N\Gamma_s P_s - \frac{\nu_s}{\nu_R} \frac{g_R}{A_{eff}} \Gamma_R P_R P_s, \quad (2)$$

$$\frac{dP_R}{dz} = [(\sigma_R^a + \sigma_R^e)N_2 - \sigma_R^a]N\Gamma_R P_R + \frac{g_R}{A_{eff}} P_s \Gamma_R (P_R + P_{spon} \kappa) - \alpha_R P_R. \quad (3)$$

Here,  $\sigma_i^a$  and  $\sigma_i^e$  ( $i = P, S$  and  $R$ ) are the absorption and emission cross sections of Yb-ions and  $N$  is total number of Yb-ions in the doped core. Furthermore,  $A$  is the Yb-doped area (typically the core area),  $\Gamma_i$  is the mode overlap with the Yb-doped area,  $A_{eff}$  is the effective area for the Raman interaction,  $\nu_s$  and  $\nu_R$  are the signal and Raman Stokes frequencies, and  $g_R$  is the Raman gain coefficient of standard single-mode germanosilicate fiber at  $\sim 1 \mu\text{m}$  ( $\sim 1 \times 10^{-13}$  m/W in case of polarized light and reduced by factor of 2 for unpolarized light).  $P_{spon}$  is the spontaneous Raman scattering power, which becomes  $\sim 177$  nW when assuming an effective Raman Stokes bandwidth of  $\sim 1$  THz and one photon is generated per mode per unit time per unit frequency.  $\kappa$  is a polarization factor ( $\kappa = 1$  for polarized light and  $\kappa = 2$  for unpolarized light). Although, depending on the operating conditions, amplified spontaneous emission (ASE) from the Yb-ions may be important, we neglect a similar spontaneous emission term resulting from the Yb-ions. Furthermore,  $\alpha_R$  is the background attenuation coefficient of the Raman Stokes wave. The point of this work has been to make  $\alpha_R$  large enough to suppress the build-up of the Stokes wave. By contrast, the background attenuation coefficients for the pump and signal waves are small, and have been neglected. Finally,  $N_2$  is the normalized excited-state population of the Yb-ions, which becomes

$$N_2 = \frac{\sigma_p^a P_p \Gamma_p / Ah\nu_p + \sigma_s^a P_s \Gamma_s / Ah\nu_s + \sigma_R^a P_R \Gamma_R / Ah\nu_R}{1/\tau + (\sigma_p^a + \sigma_p^e) P_p \Gamma_p / Ah\nu_p + (\sigma_s^a + \sigma_s^e) P_s \Gamma_s / Ah\nu_s + (\sigma_R^a + \sigma_R^e) P_R \Gamma_R / Ah\nu_R}. \quad (4)$$

Here,  $\tau$  is the fluorescence lifetime of the Yb-ions and  $h$  is Planck's constant.

Though Eqs. (1) – (4) are for the steady state, they can also be used in the quasi-steady state. In our case the pulse energy will be on the  $\mu\text{J}$  level, which is low compared to the intrinsic saturation energy of a typical single-mode YDFA ( $\sim 10 \mu\text{J}$  or more). In this situation, in the interaction with the Yb-ions described by Eq. (4), the average power of the signal should be used. However, the Raman interaction is near-instantaneous, so for that, the peak powers must be used. The Yb-induced amplification described by Eqs. (2) – (3) applies to both instantaneous

and average power. Hence, the peak power, rather than the average powers, should be used in Eqs. (2) – (3). The pump is cw, and its cw power should be used in Eq. (1).

The Raman Stokes power is generally dependent on the signal intensity and the fiber loss at the Stokes wavelength ( $\alpha_R$ ) from Eq. (3). Therefore, the design approach for SRS suppression is to either choose a larger core fiber, e.g., a low-NA large mode area (LMA) fiber [12], which increases the effective area, or enhance the loss at the Stokes wavelength without any additional loss at the signal wavelength. We have selected the second option, and designed the core structure in such a way that the propagation loss at the Raman Stokes wavelength will be high while the loss at the signal wavelength will remain low. We have used a W-type fiber, which only guides light with wavelengths shorter than the cut-off wavelength of the fundamental LP<sub>01</sub> mode [13]. Light above that wavelength escapes from the core. The interaction between the core or light guided in the core with any un-guided light is drastically reduced. W-type fibers have been used in the past few years for Nd-doped double-clad fiber lasers at around 930 nm [14-15]. These require that emission from the competing unwanted 1060 nm transition is suppressed. Similarly, a W-type fiber designed for appropriate LP<sub>01</sub> cut-off wavelength can effectively suppress SRS.

Although a W-type fiber does have a well-defined fundamental-mode cut-off in theory, the practical cut-off is less well defined. This is particularly so since the effective index of the mode, which becomes lower than the refractive index of the cladding for wavelengths beyond the cut-off, varies quite slowly with wavelength near the cut-off. Furthermore, in a double-clad fiber, the mode remains guided by the inner cladding even beyond the cut-off wavelength of the core structure. The overlap of the fundamental mode with the core decreases significantly even before the theoretical cut-off wavelength is reached due to an increasing mode field diameter. The gradual decrease continuous beyond the cut-off. The details depend on the geometry of the inner cladding. In addition, as the mode field diameter increases near cut-off, mode-coupling and micro-bend loss to cladding-modes become significant in double-clad fibers. This spreads the light out among modes of the inner cladding. In our case the inner cladding area is over 1000 times larger than the core area, so further interaction with the core becomes negligible. Thus the light is effectively lost from the core.

In practice, bending, including micro-bending, would shift the effective cut-off to a shorter wavelength, and increase the loss at a fixed wavelength, without any change of the qualitative behavior. With or without bending there is a gradual increase with wavelength of loss from the core to the surrounding inner cladding, rather than a sharp cut-off. This justifies the use of a simple loss coefficient for the Stokes wave, on both sides of the cut-off wavelength, instead of a more complex, but probably not more accurate, analysis of the modal fields and mode-coupling. Experimentally, we will optimize the performance of the amplifier by bending the fiber, to induce as large as possible loss for the Stokes wave, but before the loss-increase at the signal wavelength start to degrade the performance.

In order to theoretically evaluate the maximum signal output power from an Yb-doped fiber amplifier, as limited by SRS, we numerically solved the coupled Eqs. (1) – (4) for the pump, signal and Raman Stokes, without considering Yb ASE. The fiber had an effective area ( $A_{eff}$ ) of 75  $\mu\text{m}^2$ , and a pump absorption of 0.3 dB/m. An Yb<sup>3+</sup> ion concentration in the core is  $1.65 \times 10^{25}$  ions/m<sup>3</sup>. The absorption cross section at the pump wavelength (980 nm) is 2.4  $\text{pm}^2$ , the absorption and emission cross section at the signal wavelength (1060 nm) is 0.005  $\text{pm}^2$  and 0.3  $\text{pm}^2$  respectively and the lifetime of Yb<sup>3+</sup> ions is 0.8 ms. An average signal power of 2 W is launched into the fiber, which is equivalent to ~600 W peak power for our 103 ps 32 MHz repetition rate pulses. We varied the power of the cw pump to evaluate the obtainable signal output power, limited by SRS. The pump and signal are co-propagating from  $z = 0$  to  $z = L$  ( $L = 23$  m is the fiber length). The Raman Stokes wave also starts to evolve from the input end of the fiber. Since the physical length of the pulses in the fiber is only 2 cm, i.e., much shorter than the fiber, SRS will only be effective in the forward-propagating direction. The pump and the signal wavelengths are 980 nm and 1060 nm respectively. The 1<sup>st</sup> order Raman Stokes appears

at 1114 nm. Raman conversion to higher Stokes orders is neglected, as we are really only interested in the regime in which the power in the 1<sup>st</sup> order Stokes wave will be small. We calculated the dispersion of the W-type fiber we consider to  $-38 \text{ ps nm}^{-1} \text{ km}^{-1}$ . This leads to a walk-off between signal and Stokes waves of 47 ps over 23 m of fiber. However, the Raman amplification will be concentrated to a smaller length of the fiber, where the signal power is high. In particular, with high loss at the Stokes wavelength, the Raman gain will be too low to overcome the loss for low signal power. This reduces the actual fiber length over which the Stokes wave builds up and over which dispersion is important. Thus, though the walk-off may reduce the interaction between signal and pump pulses somewhat, the effect should be small, and is neglected in our steady-state analysis.

The intrinsic background attenuation coefficient at 1114 nm, induced by material scattering and impurity absorption, is taken to be 0.01 dB/m. This value is in line with losses measured in double-clad Yb-doped fiber, and is much lower than what will be required to suppress SRS. The mode overlap factors of the signal and Raman Stokes ( $\Gamma_s, \Gamma_R$ ) are approximated to unity. For the signal, we estimate the overlap factor to 0.77, but the difference this makes will not be significant compared to the impact of other factors such as uncertainties in dopant concentrations and cross-sections. More interesting for us is the variation of the mode area of the Stokes wave near the cut-off wavelength. For our fiber, at the theoretical cut-off of 1110 nm, the overlap with the Yb-doped raised-index core, is as low as 0.06. However, at the Stokes wavelength of 1114 nm, the calculated overlap becomes smaller of 0.03, which we approximate by unity. Note that because of uncertainties of the fiber parameters, it is unclear how close to the cut-off wavelength we actually are, and hence what the over overlap would be in the actual fiber. The effective area for the Raman interaction similarly depends on the wavelength, and indeed by the bending if this distorts the mode profile, but also these effects are neglected. Figure 1 shows a simulation of the power evolution of the signal and Stokes waves for  $\alpha_R = 0.0023 \text{ m}^{-1}$  (0.01 dB/km). The 1060 nm signal peak power reaches 5.56 kW but subsequent SRS leads to complete depletion of the signal.

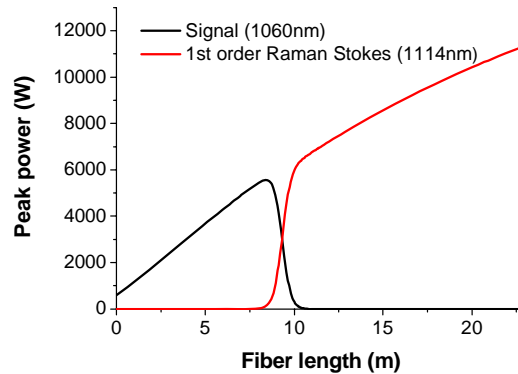


Fig. 1. Simulated power evolution of the signal and the Raman Stokes wave in our Yb-doped fiber, in the absence of Raman suppression. Absorbed pump power: 40 W (launched pump power : 70 W), input signal: 2 W average power in 103 ps pulses at 32 MHz repetition rate.

In Fig. 1, the maximum signal power coincides with the initial rise of the Stokes wave. The maximum signal power is SRS-limited, which is normally the case for us. As this maximum is associated with the rapid growth of Stokes power, we can also define it to be the Raman threshold. However, there are many exceptions to this situation: If SRS is completely

suppressed, the maximum signal power will be reached in the fiber output end, without reaching Raman threshold. In other cases, the loss at the Stokes wavelength can be so large that when the Stokes wave builds up and depletes the signal, the Raman gain and also the Stokes power drops back before the Stokes power reaches the signal power. In this case, we can still use our definition for Raman threshold, whereas the conventional definition of Raman threshold (or critical power), where the Stokes and signal output powers are equal [16-17], breaks down. We note though that with sufficiently high pump power, the Yb-gain would be high enough for the signal power to grow even after the Stokes power exceeds the signal power. In this regime, which we reached neither in experiments nor in simulations, another definition of the threshold power should be used.

We also point out that in order to reach the maximum power of 5.56 kW in Fig. 1, the fiber length would have to be cut. This however would not represent a practical amplifier, as the pump absorption would be only 2 dB. For good pump absorption and efficient operation, this particular fiber should be at least 20 m, and preferably significantly longer. For such long fibers, the peak output power (i.e., Raman threshold with our definition) that could be reached in the absence of any SRS suppression would be significantly lower. In practice this regime would be reached by operating with a higher repetition rate or a lower pump power. The benefits of SRS suppression would be greater with the longer fiber length required for efficient, practical, operation of a strictly single-mode fiber amplifier, as the suppression would act over a longer length of fiber.

Figure 2 shows the maximum peak signal power (Raman threshold) and the fiber length at which the corresponding power is reached vs. loss at the Stokes wavelength in a Yb-doped fiber amplifier operating at 1060 nm. The maximum power increases linearly with the loss at Stokes wavelength, as SRS is suppressed. A loss of 20 dB/m at the Stokes wavelength allows for a fiber length of 21 m and a peak output power of 11 kW, before SRS begins to deplete the signal. Note that whereas the simulations extended over 23 m of fiber, the fiber would have to be terminated at the maximum signal power to avoid severe SRS in the remaining fiber, as illustrated in Fig. 1.

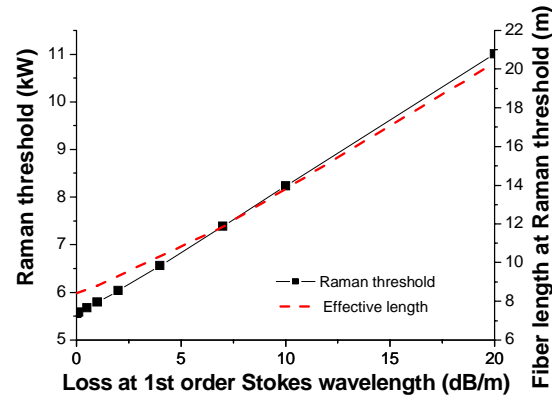


Fig. 2. Calculated maximum signal power (Raman threshold) and the fiber length at corresponding power vs. loss at the Raman Stokes wavelength. Launched pump power 70 W, pump absorption 0.3 dB/m, input signal, 2 W average power in 103 ps pulses at 32 MHz repetition rate).

### 3. SRS-suppressing fiber design

A W-type fiber was designed for a fundamental mode ( $LP_{01}$ ) cut-off between 1060 nm and 1114 nm. The core structure consists of a 7  $\mu\text{m}$  diameter core, and a 7  $\mu\text{m}$  thick depressed clad. The index difference ( $\Delta n$ ) of the doped core and the depressed clad are 0.003 and -0.002

respectively, both with respect to the silica outer cladding ( $n_{\text{silica}} = 1.45$ ). The effective indices of the two lowest-order modes ( $\text{LP}_{01}$  and  $\text{LP}_{11}$ ) were calculated using the above fiber parameters based on a weakly guiding approximation and linearly polarized modes as presented in reference [14]. As shown in Fig. 3(a), the  $\text{LP}_{01}$  mode cut-off wavelength where the effective index ( $n_{\text{eff}}$ ) became equal to the silica cladding index ( $n_{\text{silica}}$ ), will be around 1.1  $\mu\text{m}$ . However, because of the subtle nature of the cut-off and uncertainties in fiber parameters, the exact theoretical value of the cut-off wavelength is of little use and even difficult to determine exactly. Furthermore, we are really more interested in the loss. Figure 3(b) shows the bending loss of our W-type fiber at different bending radii near the  $\text{LP}_{01}$  mode cut-off wavelength, calculated with a commercial software package (Fiber\_CAD 1.5, Optiwave Systems). Here, we can see an actual  $\text{LP}_{01}$  mode cut-off at  $\sim 1.16 \mu\text{m}$  for the bending radius of 30 cm, where the loss starts to increase significantly. Moreover, the effective  $\text{LP}_{01}$  mode cut-off shifts to shorter wavelengths by additional bending. At a bending radius of 10 cm, the bending loss becomes as high as 20 dB/m at 1114 nm, while the bending loss at 1060 nm remains below 1 dB/m. In a double-clad fiber, light at the Stokes wavelength would quickly leak out from the core into the inner cladding, while 1060 nm signal light is maintained as a well-confined single mode in the core.

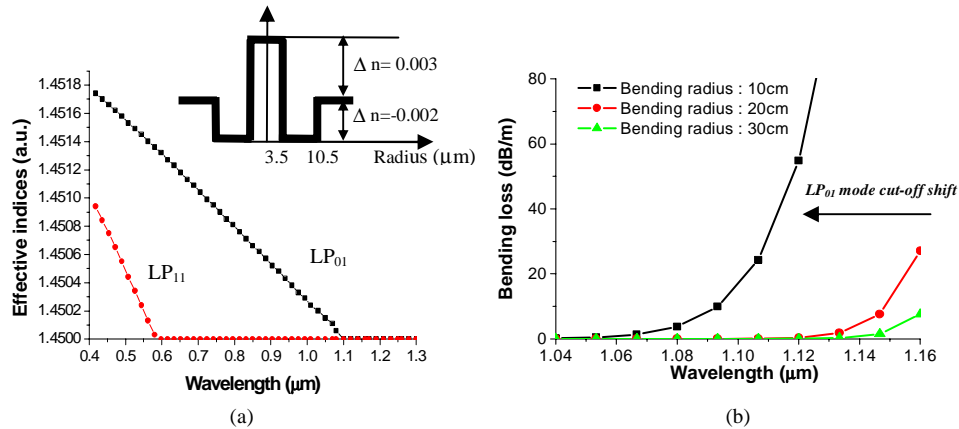


Fig. 3. (a) Effective indices vs. wavelength of the W-type fiber we designed. Inset: Core structure. (b) Calculated  $\text{LP}_{01}$  mode bending loss of the designed W-type fiber versus wavelength at different bending radii.

#### 4. Experiment and results

An Yb-doped W-type fiber preform was fabricated in house using a standard MCVD and solution doping technique. The preform was further jacketed in order to increase the inner cladding size, for efficient pump coupling into the fiber from a highly multimode diode pump source, whilst maintaining single-mode core dimensions. The preform was milled to a D-shape in order to maintain a uniform pump absorption along the fiber. The preform was then drawn to a fiber of inner-cladding diameter 370  $\mu\text{m}$  and coated with a low-index polymer outer cladding, which provides a nominal inner-cladding NA of 0.48. The fiber has a core diameter of 7  $\mu\text{m}$ , with a depressed ring in the inner cladding of thickness 7  $\mu\text{m}$ . The core and the depressed cladding index differences are effectively 0.003 and -0.002 respectively, both with respect to the silica inner cladding. The fiber parameters match those of our modal calculations described in the previous section. The small signal absorption at the pump wavelength, 975 nm, was  $\sim 0.3$

dB/m. Figure 4(a) shows core transmission spectra of this fiber, measured at different bend radii with a spectrally flat white light source. From this, the actual effective  $LP_{01}$  mode cut-off wavelength can be estimated as the wavelength where the loss in the fiber is 5 dB/m [18]. Figure 4(b) shows the resulting cut-off wavelengths. It becomes 1157 nm for a straight 1 m long fiber. This value is slightly different from our calculation, which we attribute to imperfections in the refractive index profile and uncertainties in parameters. In general, though, the fabricated fiber matched well with our expected  $LP_{01}$  mode cut-off characteristics and with additional bending the cut-off wavelength can be shifted further to shorter wavelengths, between the signal and Stokes wavelengths. However we emphasize that it is really the loss spectrum rather than the cut-off wavelength that is of interest. Figure 4(a) shows that when the fiber is coiled to a radius of 7 cm, the bend-loss at 1060 nm remains small while it becomes 5 dB/m at 1114 nm.

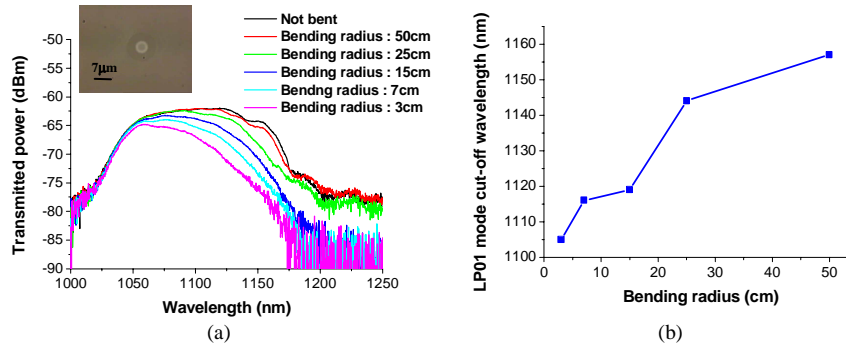


Fig. 4. (a) White light transmission spectra for different bend radii of the fabricated fiber measured with a tungsten-halogen lamp. Fiber length 1 m, spectral resolution 1 nm. Inset: back-lit image of our W-type fiber. (b)  $LP_{01}$  mode cut-off vs. bend radius.

The W-type fiber was incorporated into a pulsed MOPA system (Fig. 5). Its peak output power would be sufficient to reach the SRS threshold, for low losses at the Raman Stokes wavelength. A 1060 nm fiber pigtailed Fabry Perot laser diode was used as a seed source. It was gain-switched at 32 MHz repetition rate and generated pulses of 103 ps duration. The average output power was 0.5 mW. The diode was first amplified to 3 W average power through three cascaded YDFAs. After transmission through a free-space isolator with 1.5 dB of insertion loss, the signal was free-space coupled into the final high-power amplifier stage. It was made with a 23 m long piece of the W-type Yb-doped fiber, cladding-pumped in a co-propagating configuration by a diode stack at 975 nm. The Yb-doped W-type fiber, used only in the final amplifier, was angle-polished at both ends.



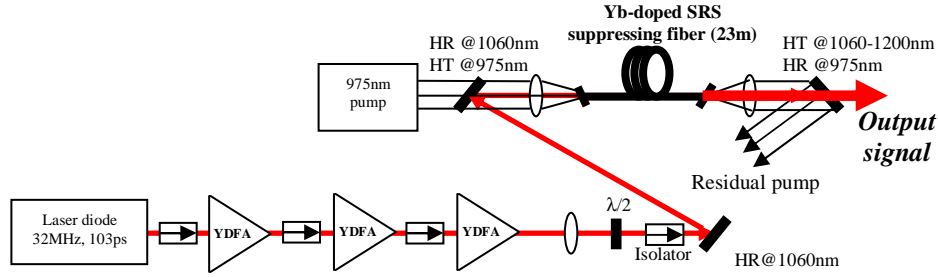


Fig. 5. Experimental MOPA set-up. HR: high reflectivity, HT: high transmission.

Figure 6 shows the average output power of the amplifier at different final-stage pump powers for fiber bending radii of 15 and 5 cm, at a constant signal input power. When the fiber was coiled to a 15 cm bending radius, the overall efficiency was 53% with respect to the absorbed pump power, while for a bending radius of 5 cm, the efficiency increased to 80%. For a 15 cm bending radius, a roll-over in the output is observed at 40 W of absorbed pump power, which indicates that the power has been transferred from the 1060 nm signal to the Raman Stokes beam. By contrast, when the fiber was coiled to a bending radius of 5 cm, the average output power increased linearly with the absorbed pump power. There was no roll-over, and the output power was limited by the available pump power.

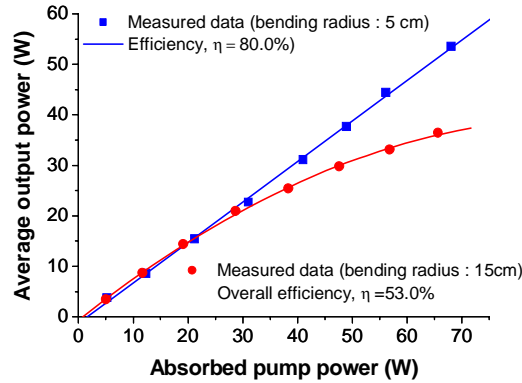


Fig. 6. Output power characteristics of the MOPA system at different bending radii.

Figure 7 shows optical output spectra measured at different pump powers. For a 15 cm bend radius, the Raman Stokes becomes significant for 66 W of absorbed pump power. In this case, although the induced loss by the fundamental mode cut-off at 1114 nm was ~2.5 dB/m, estimated from Fig. 4(a), the suppression of SRS was not enough. By contrast, no power has been observed in the Raman Stokes for a bending radius of 5 cm, even at the maximum pump power. This is because of the higher loss at 1114 nm.

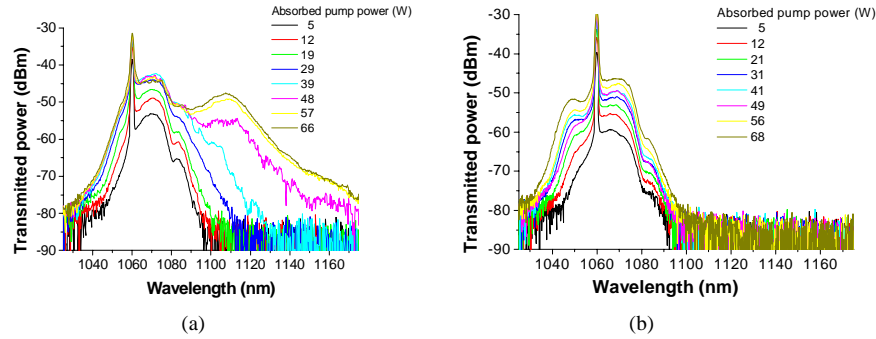


Fig. 7. Optical output spectra of the MOPA system. (a) bending radius 15cm, (b) bending radius 5cm. Resolution 1 nm.

Figure 8 shows the fractions of the total power in the signal at 1060 nm, the Yb ASE, and the Raman Stokes beam, respectively. In order to see the fraction of each power component, the output spectra in Figs. 7(a) and 7(b), on a linear scale, were fitted by four Gaussian shaped function. Their center wavelengths, peak heights and widths were found through a least-square fitting procedure for each spectrum. Good fits were obtained. The integrated power, in the different peaks were calculated, and attributed to the signal (1060 nm peak), Yb ASE (1050 nm, 1070 nm peaks) and 1<sup>st</sup> order Raman Stokes (1114 nm peak). The fiber with the bending radius of 15 cm suffered significantly from energy transfer to both Yb ASE at the longer wavelength (~1070 nm) and the Raman Stokes at 1114 nm. It can be seen from Fig. 8(a) that only 48% of the total power is at 1060 nm at the maximum pump power. On the other hand, when the fiber was coiled to 5 cm bending radius, the signal power increases linearly with respect to the pump power and 81% of the total power remains at 1060 nm at the maximum pump power, which corresponds to a peak power of 13 kW. Interestingly, the spectral filtering induced by the bending is sharp enough to also suppress ASE. This is important, since in this regime with our pulse parameters the dominant loss mechanism is ASE, according to Fig. 8(a). We note that ASE is bi-directional, with most power normally emitted towards the pump launch, i.e., signal input end of the fiber. We did not monitor backward-propagating power, but this could explain the reduction in forward output power seen in Fig. 6 with 15 cm bend radius. In our case, however, SRS as well as ASE from the earlier amplifier stages would enhance the ASE in the forward direction, but not in the backward direction. Thus, the influence of the backward ASE remains uncertain. Finally we point out that at higher peak powers, SRS rather than ASE would become the dominant loss mechanism, but they can both be mitigated significantly using a W-type core structure with a fundamental mode cut-off.

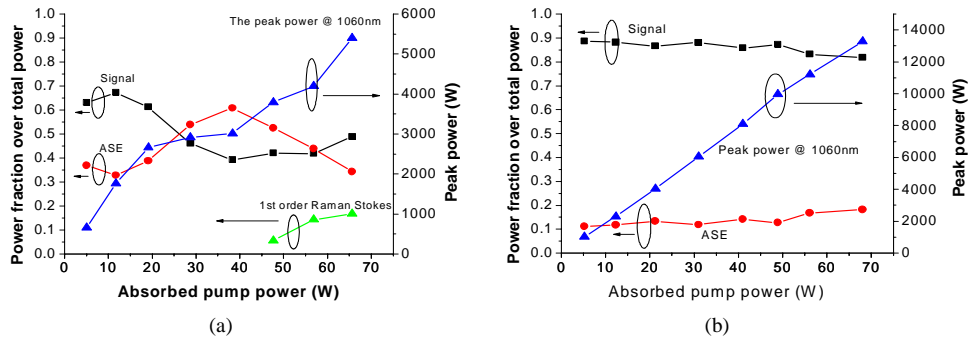


Fig. 8. The ratio of the signal, the Yb ASE and the Raman Stokes power over the total output power in the forward direction and the corresponding signal peak power at 1060 nm. (a) bending radius 15 cm, (b) bending radius 5 cm.

## 5. Conclusion

We experimentally demonstrated ASE and SRS suppression in a pulsed high power, Yb-doped, single-mode fiber MOPA system using a W-type fiber with fundamental ( $LP_{01}$ ) mode cut-off. By applying bending to the fiber a loss at the Stokes wavelength could be created, which suppressed the build-up of the Stokes wave and even of ASE quite close to the signal wavelength (1060 nm). The Stokes wavelength was effectively cut off. With this SRS suppressing W-type fiber in the final-stage amplifier, we generated 53 W of average output power with 103 ps pulse width at 32 MHz repetition rate, which corresponds to 13 kW peak power. This power was limited by available pump power. There was no power at the Raman Stokes wavelength in the output beam and Yb ASE at longer wavelength was also significantly mitigated by the additional loss at those wavelengths. By contrast, when the fiber was kept straight, the loss at the Raman Stokes wavelength was insufficient to suppress SRS and Yb ASE, and the peak power dropped to only 5.4 kW.

Even though our W-type fiber cannot reach the peak powers that have been reported from large core fibers, an important practical advantage is the robust single-mode output that results from the use of a strictly single-mode core. A W-type fiber design looks promising for scaling up the output power of both CW and pulsed fiber based sources while maintaining a robust single-mode output beam.

## Acknowledgment

We thank our colleague, Carl Farrell, for useful discussions and advice.